

## MONOTONIC BEHAVIOR OF GEOTEXTILE REINFORCED SOILS UNDER DISCRETE ROTATION OF PRINCIPAL STRESSES\*

M.R. HABIBI<sup>1</sup>, A. SHAFIEE<sup>2\*\*</sup> AND M.K. JAFARI<sup>3</sup>

<sup>1</sup>Islamic Azad University, Science and Research Branch, I. R. of Iran Tehran

<sup>2</sup>IIEES, Los Angeles, United States

Email: alishafiee6572@gmail.com

<sup>3</sup>IIEES, I. R. of Iran

**Abstract**— Monotonic triaxial compression, triaxial extension and torsional shear tests were carried out on geotextile reinforced sand and reinforced clay, mainly to investigate the effects of rotation of principal stresses on the mechanical behavior of the reinforced soil materials. The tests were carried out on unreinforced and reinforced specimens with 2, 3 and 4 geotextile layers under three different confining pressures. Investigation of the monotonic behavior of the reinforced materials under different stress paths, i.e. triaxial compression, triaxial extension, and torsional shear shows that direction of principal stresses can have profound effects on the stress-strain curve, shear strength, and slope and intercept of failure envelope. Test results reveal that geotextiles improve the mechanical properties of the sand and clay, since both strain at failure and undrained shear strength increase with the number of geotextile layers in sand and clay. In addition, test results indicate that geotextile inclusion enhances the mechanical properties of geotextile reinforced sand and clay, however, geotextiles seems to be more effective when used to reinforce sands.

**Keywords**— Principal stress rotation, geotextiles, sand, clay

### 1. INTRODUCTION

Reinforcement with geosynthetics has gained in popularity due to its versatile applications in various problems such as retaining walls, pavements, foundations, and embankments [1]. With regard to the cost of the in situ tests on geosynthetic reinforced soils, there is more tendency to use physical modeling in different scales, however, in some cases, element testing like monotonic/cyclic triaxial [2-4] have been carried out to qualitatively evaluate the mechanical behavior of geosynthetic reinforced soils.

Geotextiles upgrade the mechanical properties of soils by three mechanisms: 1-enhancing the bonds in the soil due to the interlocking of the soil particles with the reinforcement apertures [5], 2-contributing to the shear resistance depending on the direction of reinforcements with respect to the failure plane [5], and 3-increasing lateral stress through limiting lateral deformations [6]. A review of the geotechnical literature of the geotextile-reinforced soils in the scale of element testing reveals that a majority of the studies have been carried out either in the triaxial device (compression loading) or in the direct shear device. The direct shear tests mainly focus on the soil-geotextile interface behavior [7-9].

Chandrasekaran et al. [10] tested polyester reinforced sands under drained triaxial conditions, and found that deviatoric stress and dilation increase with the number of polyester layers. Krishnaswamy and Isaac [11] found that liquefaction resistance of saturated sands significantly increases with the number of

\*Received by the editors July 28, 2013; Accepted December 28, 2013.

\*\*Corresponding author

geotextile layers. Haeri et al. [2] performed triaxial compression tests on unreinforced and geotextile reinforced saturated sandy specimens. The results demonstrated that geotextile inclusion increases the peak strength, axial strain at failure, and ductility, however, it reduces dilation. Failure envelopes for the reinforced sand were observed as bilinear or curved. Latha and Murthy [12] showed that geotextile reinforced dry sands exhibit cohesion in triaxial compression. The cohesion increases with the number of geotextile layers. Moghaddas Tafreshi and Asakereh [13] demonstrated that strength of the geotextile reinforced silty sands increases nonlinearly with confining pressure in such a manner that at high confining pressures the reinforcement is not effective.

As a result of the growing interest in utilizing on-site cohesive soils in reinforced soil structures associated with significant cost reduction, the research on the subject of the mechanical behavior of geotextile reinforced clays has been intensified (e.g., [7,14]). Ingold [15] performed a limited number of tests on partly saturated clay with impermeable reinforcement. The results revealed that the strength is reduced in clay with high degree of saturation. Ingold and Miller [16] found that the drained shear strength and secant deformation modulus of the reinforced clay increase with the decrease in spacing between the layers of reinforcement. Ling and Tatsuoka [17] demonstrated that enhanced confinement is offered to the geotextile reinforced clay when it is consolidated anisotropically. Unnikrishnan et al. [3], by the help of monotonic compression and cyclic triaxial tests, showed the enhancement of strength and deformation properties of geotextile reinforced clays through using a thin layer of high-strength sand provided on both sides of the reinforcement. Mofiz ad Rahman [1] showed that reinforced clayey soils exhibit higher failure strains and volume contraction than unreinforced soils under drained triaxial condition. Noorzad and Mirmoradi [4] carried out unconsolidated undrained tests on geotextile reinforced clays. They showed that moisture content, relative compaction and number of geotextile layers affect the strength properties of reinforced soils. They found that peak strength increases with relative compaction and number of geotextile layers, and decreases with moisture content.

On the other hand, in the field, soil elements undergo different loading paths depending upon the loading conditions. It is well known that mechanical properties of sands and clays are highly dependent on the principal stress rotation. There exists a number of studies that show how drained and undrained behavior of sands is affected by rotation of principal stresses. Arthur et al. [18] tested dense and loose sands in the directional shear device, and showed that drained shear strength decreases with  $\alpha$  (defined as the angle between major principal stress and vertical axis), while effective friction angle is not affected remarkably by the rotation of principal stress axes. Symes et al. [19] showed how pore pressure build-up in sands is affected by rotation of principal stresses at constant shear stress. It was found that excess pore pressure increases and deviatoric stress decreases when  $\alpha$  is increased. They revealed that accumulation of pore pressure during cyclic principal stress rotation may even lead to failure. Yoshimine et al. [20] made it clear that the sand exhibits highest resistance with lowest contractancy in triaxial compression ( $\alpha = 0^\circ$ ), while triaxial extension ( $\alpha = 90^\circ$ ) gives the opposite extreme in the assessment of flow failure.

The mechanical behavior of clayey soils is also affected by rotation of principal axes. Hicher and Lade [21] found that stress-strain behavior and pore pressure are affected by principal stress rotation, and strength and pore pressure developments occur faster in monotonic tests without stress rotation. Hight et al. [22] tested Bothkennar clay under triaxial compression, triaxial extension and simple shear conditions and found that the highest undrained shear strength is obtained in triaxial compression, while the lowest one is attained in triaxial extension. Albert et al. [23] conducted a series of laboratory tests to evaluate the effect of the continuous rotation of principal stresses on Bothkennar clay and found that the effective

stress paths are not as brittle as those observed in triaxial compression tests. In addition, failure of all specimens occurred when  $\alpha$  reached, on average,  $33^\circ$ . Lade and Kirkard [24] performed a series of consolidated-undrained torsion shear tests on the  $K_0$ -consolidated specimens of San Francisco Bay Mud. It was shown that the undrained shear strength decreases systematically with inclination of the major principal stress, from triaxial compression with  $\alpha = 0^\circ$  to triaxial extension with  $\alpha = 90^\circ$ . Lin and Penumadu [25] presented the effective friction angles, undrained shear strengths, stress-strain relationships, pore water pressures and stress-paths as a function of the angle of principal stress rotation.

The present study aims to determine the effect of rotation of principal stresses on the monotonic behavior of geotextile reinforced sand and clay. The monotonic tests have been conducted on the isotropically confined specimens under triaxial compression (TC), triaxial extension (TE), and torsional shear (TS) conditions. Figure 1 shows the total stress path in each of the tests. Herein,  $p$  and  $q$  represent the mean and deviatoric total stresses respectively, and are obtained by:  $p = \frac{\sigma_1 + 2\sigma_3}{3}$ , and  $q = \sigma_1 - \sigma_3$  where  $\sigma_1$  and  $\sigma_3$  are major and minor principal stresses respectively. The sand and clay were reinforced with multi layers of geotextiles, and tested under different confining pressures.

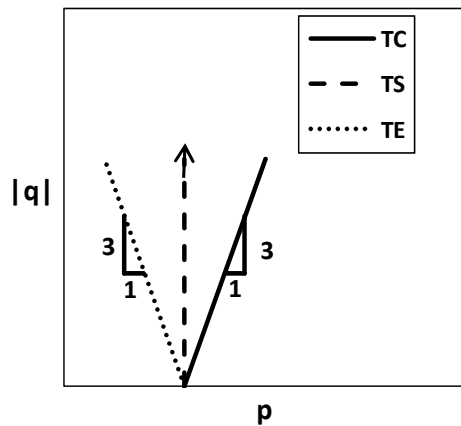


Fig. 1. Total stress path in different tests performed in this study

Although all the element tests performed in this study can be regarded as small scales physical model tests, since the thickness (and consequently the tensile strength) of the geotextiles has not been decreased in the model tests, the results should be investigated qualitatively. As Viswanadham and Mahajan [26] mentioned, two requirements should be met in order to model reinforcement layers correctly: (1) scaling of tensile strength-strain behavior and (2) modeling of the bond between soil and geotextile.

## 2. TEST MATERIALS

A silica sand and commercial clay were selected to be reinforced with geotextile to investigate the effects of principal stress rotation on the mechanical behavior of granular and cohesive soils. The sand was retrieved from a mine 60 km north of Tehran, Iran. It is a uniformly graded silica sand with a mean grain size,  $D_{50}$  of 0.25 mm, coefficient of uniformity,  $C_u$  of 1.75 and a specific gravity of 2.67. Its grains are sub-angular to sub-round in shape. It has a maximum and minimum void ratio of 0.82, and 0.43 respectively. The commercial clay had a specific gravity of 2.70, liquid limit of 42%, plasticity index of 18%, a maximum dry unit weight of 1.92 gr/cm<sup>3</sup>, and an optimum water content of 23% [27]. Two, three or four layers of a woven geotextile produced from polypropylene were interfaced between the soil layers. The properties provided by the manufacturer are given in Table 1.

Table 1. Properties of the geotextile used in this study

Physical Properties					
Fabrication process		Weight (gr/m <sup>2</sup> )		Normal thickness (mm)	
Woven		200		1.2	
Mechanical Properties					
C.B.R Puncture (N)	Max. Tensile strength (kN/m)		Max. Elongation (%)		Puncture resistance (N)
	Longitudinal	Transverse	Longitudinal	Transverse	
900	12	12	>50	>50	420

### 3. EXPERIMENTAL PROGRAM

Triaxial compression, triaxial extension and hollow cylinder torsional shear tests were performed to investigate the effects of principal stress rotation on the monotonic behavior of geotextile reinforced sand and clay. If  $\alpha$  is the angle of major principal stress ( $\sigma_1$ ) with vertical axis, then it would be  $0^\circ$ ,  $90^\circ$ , and  $45^\circ$  under triaxial compression, triaxial extension, and torsional shear conditions respectively, for an isotropically confined specimen. Figure 2 shows how the direction of major principal stress in torsional shear test makes an angle equal to  $45^\circ$  with the vertical axis. All the tests were performed under unconsolidated undrained conditions at three different confining pressures of 100, 300, and 500 kPa. Various arrangements of geotextiles were used in this study (Fig. 3). The sand/clay were reinforced with either 2, 3, or 4 layers of geotextile. Clean sand and pure clay specimens were also tested to provide a basis for the comparison of the test results. A total of 72 triaxial compression, triaxial extension, and hollow cylinder torsional shear tests were performed.

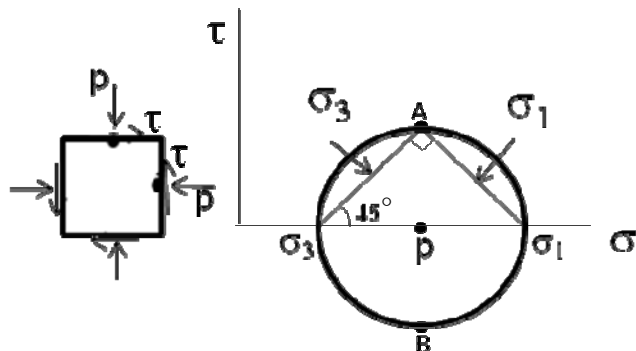


Fig. 2. Principal stress direction for torsional shear test on an isotropically confined specimen  
( $p$  =confining pressure, and  $\tau$  =shear stress)

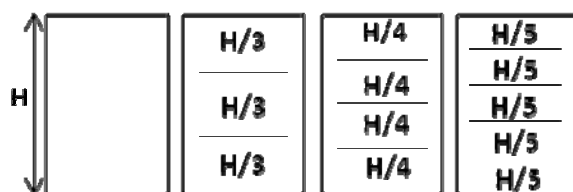


Fig. 3. Geotextile arrangements used in this study

The samples were compacted in several layers until achieving the target density. The sandy specimens were compacted with a relative density of 70% and a water content of 3%. The clayey samples were also compacted at a dry unit weight equal to 95 % of their maximum dry unit weight ( $\gamma_{d,max}$ ) and with an

optimum water content obtained from compaction test (ASTM D698, 2012). After compacting and leveling each layer of soil, the reinforcement was placed horizontally in the specimen. The diameter of the reinforcement was slightly less than that of the specimen. The number of layers for preparation of the specimen was selected between 2 and 4 depending on the geotextile arrangement. The triaxial specimens had a diameter, and height of 5 cm, and 10 cm respectively. The specimens tested in the hollow torsional device had an outside diameter of 10 cm, inside diameter of 5 cm, and a height of 10 cm. All the tests, either triaxial or torsional shear were conducted under strain-controlled conditions. The strain rate was 0.3% /min in triaxial tests, and the tests were continued up to a strain level of 15%. Corrections such as membrane penetration, membrane force, cell expansion, and cross-sectional area were considered and applied in the calculations. In hollow cylinder torsional shear tests, the rotation rate was 0.005 rad/min, and the tests were continued until achieving shear strains as high as 25%.

#### 4. TEST RESULTS AND DISCUSSIONS

##### a) Stress-strain behavior of geotextile reinforced soils

Figures 4 to 6 present stress-strain curves of the reinforced sand and clay under triaxial compression, torsional shear, and triaxial extension at different confining pressures ( $p_0$ ) respectively. Vertical axis in all the triaxial tests (Figs. 4 and 6) is deviatoric stress, which is equal to  $(\sigma_1 - \sigma_3)$ . The vertical axis in torsional shear tests (Fig. 6) is shear stress on the horizontal plane as shown in Fig. 2. As seen, in triaxial compression (Fig. 4), where  $\alpha = 0^\circ$ , geotextiles (GT) have no remarkable effects on the stress-strain curves until axial strains as high as 2%. Then, deviatoric stress increases with the number of geotextile layers. On the other hand, when  $\alpha$  increases, i.e. in torsional shear and triaxial extension, geotextiles show their reinforcing effects on the stress-strain curves, almost from beginning of the loading (Figs. 5 and 6). The geotextile reinforced sand and clay exhibit brittle behavior under all types of loading patterns, and strain at failure (where peak deviatoric stress occurs) increases with the geotextile layers.

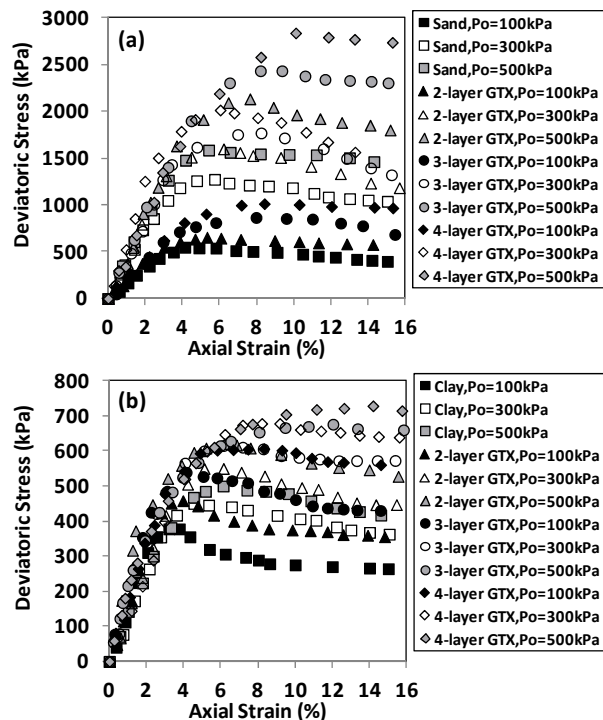


Fig. 4. Stress-strain curves under triaxial compression test (a) reinforced sand, (b) reinforced clay

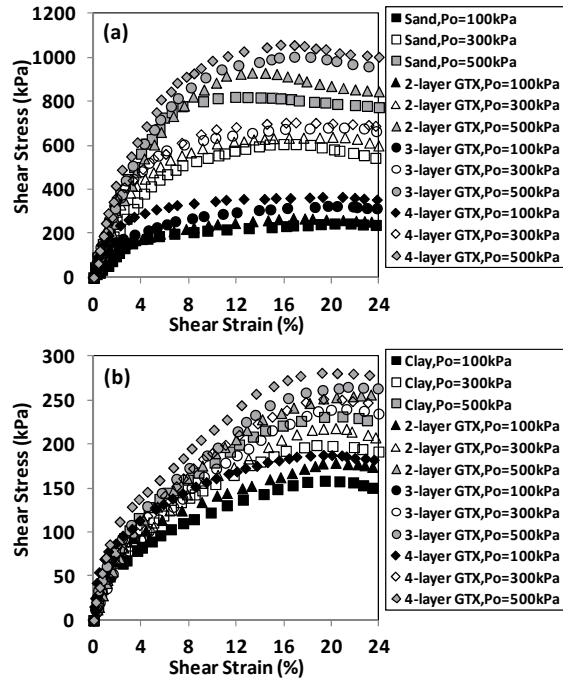


Fig. 5. Stress-strain curves under torsional test (a) reinforced sand, (b) reinforced clay

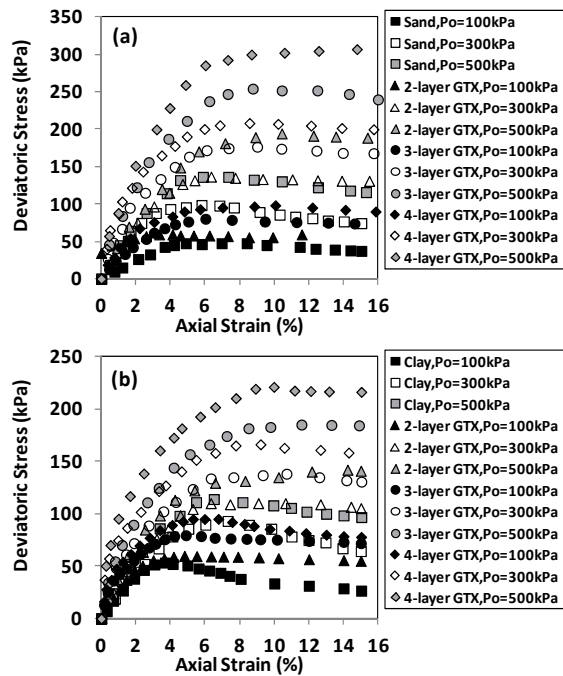


Fig. 6. Stress-strain curves under triaxial extension test (a) reinforced sand, (b) reinforced clay

### b) Undrained shear strength of geotextile reinforced soils

Undrained shear strength ( $S_u$ ) for specimens in triaxial compression and extension tests is obtained as the maximum value of the deviatoric stress ( $q$ ) from Figs. 4 and 6. On the other hand, as shown in Fig. 2, for torsional shear test on a specimen under isotropic confining pressure, the value of deviatoric stress is:  $q = \sigma_1 - \sigma_3 = 2\tau$  where  $\tau$  is the shear stress on the horizontal plane, i.e. the vertical axis in Fig. 5. Consequently,  $S_u$  will be two times the maximum value of the shear stress obtained from Fig. 5. As

shown in Fig. 7,  $S_u$  decreases with  $\alpha$  so that  $S_u$  in reinforced sand and clay is highest in triaxial compression, and lowest in triaxial extension. In general,  $S_u$  of the reinforced sand is higher than that of reinforced clay. Figure 8 presents the effects of geotextiles on the undrained shear strength of sand and clay respectively. Herein, undrained shear strength of reinforced material ( $S_{u,\text{Reinf.}}$ ) is normalized to the undrained shear strength of unreinforced material ( $S_{u,\text{Unreinf.}}$ ). The ratio is computed at each confining pressure, and then averaged over all the confining pressures. As seen, shear strength increases with the number of geotextile layers irrespective of the test type or parent material. However, geotextile is more beneficial when used in sands, and the value of  $S_{u,\text{Reinf.}}/S_{u,\text{Unreinf.}}$  in the reinforced sand is higher than that of reinforced clay. This shows that the bond strength between the sand and geotextile is higher than that of the clay and geotextile.

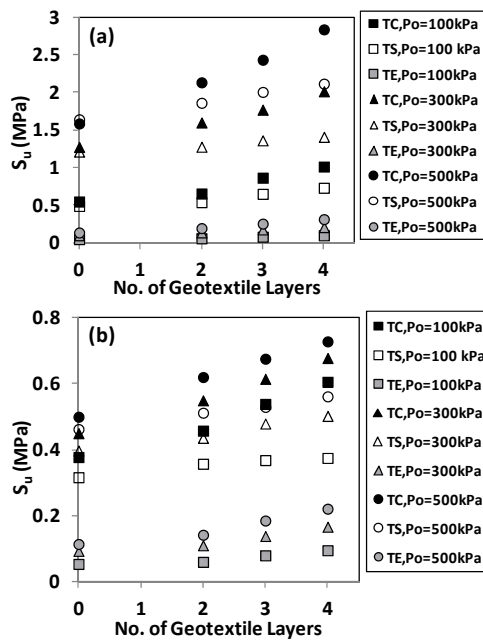


Fig. 7. Undrained shear strength in (a) reinforced sand, and (b) reinforced clay

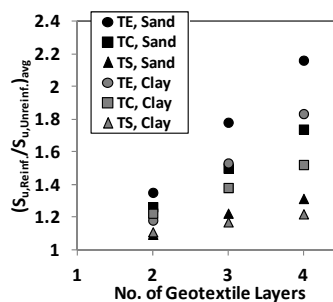


Fig. 8. Effect of geotextiles on the undrained shear strength of sand and clay for three different types of test

Figure 9 presents the effect of confining pressure on the undrained shear strength of the geotextile reinforced sand and clay respectively. Herein, undrained shear strength at each confining pressure ( $S_{u,p}$ ) has been normalized to the undrained shear strength at lowest confining pressure, i.e. 100 kPa ( $S_{u,p=100\text{kPa}}$ ). The ratio has been computed for each specimen, and then averaged over all the specimens at that particular confining pressure. As seen, shear strength increases linearly with confining pressure irrespective of  $\alpha$  or parent material. In geotextile reinforced sand,  $S_{u,p}/S_{u,p=100\text{kPa}}$  does not depend on  $\alpha$ , however, in reinforced clays,  $S_{u,p}/S_{u,p=100\text{kPa}}$  increases with  $\alpha$ . In addition, increasing confining

pressure leads to more shear strength increase in reinforced sands than clays. For instance,  $S_{u,p}/S_{u,p=100\text{ kPa}}$  reaches as high as 3.2 in the reinforced sand when confining pressure is 500 kPa, while the ratio reaches to 2.3 in the reinforced clay under the same conditions.

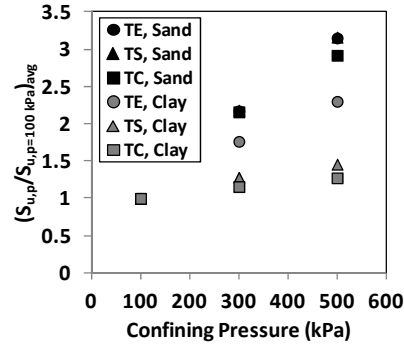


Fig. 9. Effect of confining pressure on the undrained shear strength of reinforced sand and clay

### c) Failure envelope of geotextile reinforced soils

Figures 10a and b show failure envelopes in terms of total stresses in  $q - p$  plane for the geotextile reinforced sand and clay respectively. Failure in all the reinforced soils happened within the soil, since no evidence of geotextiles failure (either ripping or pulling out) was captured during and after the tests. As seen, failure envelopes are almost non-linear, and the lowest failure envelopes belong to the triaxial extension tests. On the other hand, failure envelopes from torsional shear tests fall above that of triaxial compression tests in geotextile reinforced sands (Fig.10a), however, the trend is reversed in the geotextile reinforced clays, and except for pure clay in which failure envelope from torsional shear and triaxial compression tests are identical, the failure envelopes from triaxial compression tests lie above that of triaxial extension tests (Fig. 10b).

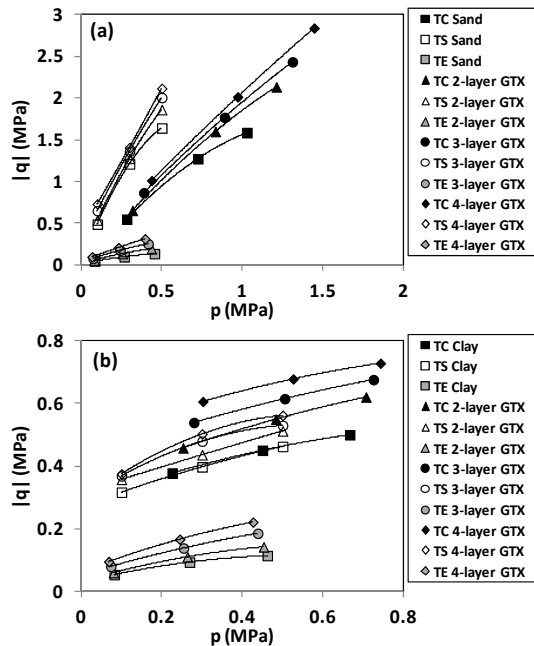


Fig. 10. Total stress failure envelopes in (a) reinforced sands, and (b) reinforced clay

In addition, it can be inferred from Fig. 10a that the slope of failure line increases with the number of geotextile layers in the geotextile reinforced sands. The slope is highest in torsional shear ( $\alpha = 45^\circ$ ) and

lowest in triaxial extension ( $\alpha = 90^\circ$ ). On the other hand, the slope of failure line in geotextile reinforced clays (Fig. 10b) does not show strong dependency on the number of geotextile layers and rotation of principal stresses. Although geotextile reinforced sands (Fig. 10a) do not show remarkable cohesion intercept (i.e. where failure line meets vertical axis), cohesion intercept increases with the number of geotextile layers and decreases with  $\alpha$  in geotextile reinforced clays. Since, the trend of variation of cohesion intercept with  $\alpha$  in the reinforced clays, and the slope of failure line with  $\alpha$  in the reinforced sand is the same as the unreinforced material (either clay or sand), one can conclude that in the types of tests (i.e., triaxial compression, triaxial extension and torsional shear) failure has occurred within the soil. A summary of the effects of rotation of the direction of principal stresses on the mechanical behavior of geotextile reinforced sand and clay is presented in Table 2.

Table 2. Effects of rotation of principal stresses on the mechanical behavior of reinforced sand and clay

Parameter/Characteristic	Geotextile reinforced sand	Geotextile reinforced clay
stress-strain curve	when $\alpha$ increases geotextiles show their reinforcing effects on the stress-strain curves from beginning of the test	when $\alpha$ increases geotextiles show their reinforcing effects on the stress-strain curves from beginning of the test
strain at failure	does not depend on $\alpha$	does not depend on $\alpha$
$S_u$	decreases with $\alpha$	decreases with $\alpha$
$S_{u,Reinf.}/S_{u,Unreinf.}$	Highest at $\alpha = 90^\circ$ , lowest at $\alpha = 45^\circ$	Highest at $\alpha = 90^\circ$ , lowest at $\alpha = 45^\circ$
$S_{u,p}/S_{u,p=100kPa}$	does not depend on $\alpha$	increases with $\alpha$
failure envelope	Highest at $\alpha = 45^\circ$ , lowest at $\alpha = 90^\circ$	moves down with $\alpha$
slope of failure line	Highest at $\alpha = 45^\circ$ , lowest at $\alpha = 0^\circ$	does not depend on $\alpha$
cohesion intercept	N.A.	decreases with $\alpha$

## 5. CONCLUSION

A laboratory study was carried out to investigate the effects of rotation of principal stresses on the mechanical behavior of geotextile reinforced sand and clay. The isotropically confined reinforced soils were tested under triaxial compression ( $\alpha = 0^\circ$ ), torsional shear ( $\alpha = 45^\circ$ ) and triaxial extension ( $\alpha = 90^\circ$ ) conditions, where  $\alpha$  is the angle between the direction of major principal stress and vertical axis. The following conclusions may be drawn based on this experimental study:

1. Geotextiles improve the mechanical properties of the sand and clay. The geotextile reinforced sand and clay exhibit brittle behavior under all types of loadings. Strain at failure and undrained shear strength increases with the number of geotextile layers in both reinforced sand and clay. In reinforced sand, slope of failure line increases with the number of geotextile layers, while in reinforced clay, cohesion intercept increases with the number of geotextile layers. In light of the increase in the undrained shear strength, strain at failure, slope of failure line (for the sand) and cohesion intercept (for the clay) with the number of geotextile layers (which is in accordance with the previous studies), and since failure has occurred within the soil, it can be concluded that the increase in aspect ratio of the soil confined between two geotextile layers, and lateral constraint provided by the geotextiles are the main causes of the enhancement of strength and stiffness properties of the geotextile reinforced soils.
2. In both geotextile reinforced sand and clay, undrained shear strength ( $S_u$ ) decreases with  $\alpha$ . In other words, the trend of variation of  $S_u$  with  $\alpha$  in the reinforced soil is the same as the parent material (either sand or clay), which means that in all types of tests (i.e., triaxial compression, triaxial extension and torsional shear) failure has occurred within the soil. In both reinforced sand

- and clay  $S_{u,Reinf.}/S_{u,Ureinf.}$  is highest at  $\alpha = 90^\circ$  and lowest at  $\alpha = 45^\circ$ . In reinforced sand  $S_{u,p}/S_{u,p=100kPa}$  does not depend on  $\alpha$ , while in reinforced clay it increases with  $\alpha$ .
3. Total-stress failure envelope depends on  $\alpha$ . Failure envelopes from triaxial extension tests are at their lowest position for both reinforced sand and clay. In reinforced sand, they are at their highest position at  $\alpha = 45^\circ$ , while in reinforced clay the highest position is achieved when  $\alpha = 0^\circ$ .
  4. Although the slope of failure line does not depend on  $\alpha$  for reinforced clay, it is highest at  $\alpha = 45^\circ$  and lowest at  $\alpha = 0^\circ$  for reinforced sand. In addition, cohesion intercept decreases with  $\alpha$  in reinforced clay.
  5. It appears that geotextiles are more beneficial when used to reinforce granular material, since parameters like  $S_{u,Reinf.}/S_{u,Ureinf.}$ , and  $S_{u,p}/S_{u,p=100kPa}$  are higher in geotextile reinforced sand compared with the corresponding values for geotextile reinforced clay. This means that sand particles exhibit better interlocking with geotextiles than the clay particles.

**Acknowledgement:** The torsional shear tests were performed at the International Institute of Earthquake Engineering and Seismology which is acknowledged.

## REFERENCES

1. Mofiz, S. A. & Rahman, M. M. (2010). Evaluation of failure load-deformation characteristics of geo-reinforced soil using simplified approach. 11th IAEG Congress, Auckland, New Zealand, pp. 4383-4392.
2. Haeri, S. M., Noorzad, R. & Oskoorouchi, A. M. (2000). Effect of geotextile reinforcement on the mechanical behavior of sand. *Geotextiles and Geomembranes*, Vol. 18, No. 6, pp. 385-402.
3. Unnikrishnan, N., Rajagopal, K. & Krishnaswamy, N. R. (2002). Behavior of reinforced clay under monotonic and cyclic loading. *Geotextiles and Geomembranes*, Vol. 20, No. 2, pp. 117-133.
4. Noorzad, R. & Mirmoradi, S. H. (2010). Laboratory evaluation of the behavior of a geotextile reinforced clay. *Geotextiles and Geomembranes*, Vol. 28, No. 4, pp. 386-392.
5. Mofiz, S. A., Rahman, M. M. & Alim, M. A. (2004). Stress-strain behavior and model of reinforced residual soil. 15th South Asian Geotechnical Society Conference, Bangkok, Thailand, pp. 607-610.
6. Broms, B. B. (1977). Triaxial tests with fabric reinforced soil. *Proc. Int. Conf. on the Use of Fabrics in Geotechnics*, Vol. 3, Ecole Nationale des Ponts et Chaussees, Laboratoire Central des Ponts et Chaussees, Paris, pp. 129-134.
7. Athanasopoulos, G. A. (1996). Results of direct shear tests on geotextile reinforced cohesive soil. *Geotextiles and Geomembranes*, Vol. 14, No. 11, pp. 619-644.
8. Lee, K. M. & Manjunath, V. R. (2000). Soil-geotextile interface friction by direct shear tests. *Canadian Geotechnical Journal*, Vol. 37, No. 1, pp. 238-252.
9. Ghazavi, M. & Ghaffari, J. (2013). Experimental investigation of time-dependent effect on shear strength parameters of sand-geotextile intersect. Iranian Journal of Science and Technology, Transactions of Civil Engineering, Vol. 37, No. C1, pp. 97-109.
10. Chandrasekaran, B., Broms, B. B., Wong, K. S. (1989). Strength of fabric reinforced sand under axisymmetric loading. *Geotextiles ad Geomembranes*, Vol. 8, pp. 293-310.
11. Krishnaswamy, N. R. & Issac, N. T. (1994). Liquefaction potential of reinforced sand. *Geotextiles ad Geomembranes*, Vol. 13, pp. 23-41.
12. Latha, G. M. & Murthy, V. S. (2006). Effects of reinforcement form on the behavior of geosynthetic reinforced sand. *Geotextiles and Geomembranes*, Vol. 25, No. 1, pp. 23-32.

13. Moghaddas Tafreshi, S. N. & Asakereh, A. (2007). Strength evaluation of wet reinforced silty sand by triaxial test. *Iranian Journal of Civil Engineering*, Vol. 5, No. 4, pp. 274-283.
14. Badv, K. & Farsimadan, R. (2009). Swelling and diffusion characteristics of the experimental GCLs. *Iranian Journal of Science and Technology, Transaction B: Engineering*, Vol. 33, No. B1, pp. 15-30.
15. Ingold, T. S. (1983). Reinforced clay subject to undrained triaxial loading. *Journal of Geotechnical Engineering*, Vol. 109, No. 5, pp. 738-744.
16. Ingold, T. S. & Miller, K. S. (1983). Reinforced clay subject to undrained triaxial loading. *Journal of Geotechnical Engineering*, Vol. 109, No. 7, pp. 883-898.
17. Ling, H. I. & Tatsuoka, F. (1994). Performance of anisotropic geosynthetic-reinforced cohesive soil mass. *Journal of Geotechnical Engineering*, Vol. 120, No. 7, pp. 1166-1184.
18. Arthur, J. R. F., Chua, K. S. & Dunstan, T. (1979). Dense sand weakened by principal stress rotation. *Geotechnique*, Vol. 29, No. 1, pp. 91-98.
19. Symes, M. J. P. R., Gens, A. & Hight, D. W. (1984). Undrained anisotropy and principal stress rotation in saturated sand. *Geotechnique*, Vol. 34, No. 1, pp. 11-27.
20. Yoshimine, M., Ishihara, K. & Vargas, W. (1998). Effects of principal stress direction and intermediate principal stress on undrained shear behavior of sand. *Soils and Foundations*, Vol. 38, No. 3, pp. 179-188.
21. Hicher, P. Y. & Lade, P. V. (1987). Rotation of principal directions in K<sub>0</sub>-consolidated clay. *Journal of Geotechnical Engineering*, pp. 113, Vol. 7, pp. 774-788.
22. Hight, D. W., Bond, A. J. & Legge, J. D. (1992). Characterization of the Bothkennar clay: an overview. *Geotechnique*, Vol. 42, No. 2, pp. 303-347.
23. Albert, C. & Zdravkovic, Jardine, R. J. (2003). Behaviour of Bothkennar clay under rotation of principal stresses. *Int. Workshop on Geotechnics of Soft Soils-Theory and Practice*. Vermeer, Schweiger, Karstunen and Cundny , eds. VGE, pp. 1-6.
24. Lade, P. V. & Kirkgaard, M. M. (2000). Effects of stress rotation and changes of b-values on cross-anisotropic behavior of natural, K<sub>0</sub>-consolidated soft clay. *Canadian Geotechnical Journal*, Vol. 40, No. 6, pp. 93-105.
25. Lin, H. & Penumadu, D. (2005). Experimental investigation of principal stress rotation in kaolin clay. *Journal of Geotechnical and Geoenvironmental Engineering*, pp. 131, No. 5, pp. 633-642.
26. Viswanadham, B. V. S. & Mahajan, R. R. (2007). Centrifuge model tests on geotextile reinforced slopes. *Geosynthetics International*, Vol. 14, No. 6, pp. 365-379.
27. American Society for Testing and Materials (ASTM). D698-12, (2012). *Standard test methods for laboratory compaction characteristics of soil using standard effort*. West Conshohocken, Pa.